

Molecular-dynamics simulations of the transport properties of a single polymer chain in two dimensions

Tapan G. Desai and Pawel Keblinski

Department of Material Science and Engineering, Rensselaer Polytechnic Institute, Troy, New York 12180

Sanat K. Kumar^{a)}

Isermann Department of Chemical and Biological Engineering, Rensselaer Polytechnic Institute, Troy, New York 12180

Steve Granick

Department of Material Science, University of Illinois, Urbana, Illinois 61801,

Department of Chemistry, University of Illinois, Urbana, Illinois 61801,

and Department of Physics, University of Illinois, Urbana, Illinois 61801

(Received 15 July 2005; accepted 2 December 2005; published online 24 February 2006)

Molecular-dynamics simulations are conducted to elucidate the critical factors affecting the transport properties of isolated polymer chains in strictly two dimensions. The relevance of surface inhomogeneity is critically examined. We unequivocally find that surface inhomogeneity is critical in obtaining transport behavior consistent with the recent measurements of surface diffusion for polymers adsorbed at the solid-liquid interface. For a systematic investigation of this point, heterogeneity was introduced by decorating the surface with impenetrable elements and we find that chain diffusivity crossed over from Rouse-type behavior to reptationlike with increasing surface coverage of obstacles. This transition in behavior occurred when the mean distance between obstacles is approximately equal to the end-to-end distance, R_e , of the two-dimensional chain. Our results underscore the importance of surface disorder (not only literal obstacles but by reasonable extension also to other types of disorder) in determining the transport behavior of chains adsorbed to solids. © 2006 American Institute of Physics. [DOI: 10.1063/1.2161197]

I. INTRODUCTION

The dynamics of polymer chains in melts and dilute solutions have been extensively studied both experimentally and by computer simulations.^{1,2} The Brownian motion of polymer chains in dilute solutions is dominated by long-range hydrodynamic interactions (Zimm regime),³ and the self-diffusion coefficient D scales as $D \sim N^{-0.6}$, where N is the degree of polymerization. This scaling can be obtained from simple considerations, i.e., by assuming that the chain moves in a solution with a hydrodynamic drag force proportional to its radius of gyration R_G , which in good solvent scales as $R_G \sim N^{0.6}$. These hydrodynamic interactions are fully screened for polymer chains in dense melts. Then, for short unentangled (Rouse regime⁴) polymer chains, $D \sim N^{-1}$, whereas for longer chains exhibiting reptation, D is expected to vary as $D \sim N^{-2}$.¹

The structure and dynamics of an adsorbed chain differ profoundly from that in the bulk. This study focuses on the center-of-mass lateral diffusion coefficient of adsorbed chains, in particular, the case in which the dilute adsorbed chain assumes a “pancake” conformation in which the size of the chain in the normal direction is independent of N . The in-plane size for such well-adsorbed chains is known in two dimensions and a good solvent environment to be $R_G \sim N^{-3/4}$. It is self-evident that D for this situation would be

zero in the case of strong, localized surface attractions, but finite otherwise. One recognizes immediately that the dynamics depend on the surface-polymer interaction and might not exhibit the degree of universality observed in the bulk. The aim of this paper is to contribute in elucidating the aspects in which the self-diffusion of polymer chains in two dimensions (2Ds), in fact, is or is not universal, i.e., the degree to which it scales in a simple way with physical variables. Seeking universality while holding constant issues relating to surface chemical interactions, we inquire into the N dependence of surface diffusion.

Although few relevant experiments have been reported, there appear to be two limiting possibilities. On one hand, Sukhishvili *et al.*⁵ measured D of dilute uncharged flexible chains adsorbed at the solid-liquid interface, finding $D \sim N^{-3/2}$. Earlier experiments by Maeir and Radler⁶ for double-stranded DNA chains adsorbed on a fluid phospholipid bilayer show a different scaling, $D \sim N^{-1}$, the in-plane chain size following the predicted scaling $R_G \sim N^{-3/4}$. Similar scaling of D with N was also found by Zhang and Granick for synthetic macromolecules adsorbed on fluid phospholipid layers.⁷ These contrasting results highlight the central role of surface structure, solid or fluid, in influencing the observed N scaling.

How to explain this major difference? In prior literature, the screening of hydrodynamic interactions was conjectured to be very different at a static (solid) surface and a dynamic (fluid) surface. It was speculated that phospholipid bilayers

^{a)} Author to whom correspondence should be addressed; electronic mail: kumar@rpi.edu

might provide an effective dissipative bath for rapid momentum transport resulting in the screening of hydrodynamic interactions, this leading to uncorrelated Rouse dynamics of the adsorbed DNA.⁶ This screening process might not take place on a solid substrate yielding the different scaling behavior.⁵ In the present paper, we do not account for the influence of hydrodynamic interactions.

In this paper we systematically test an alternative explanation suggested by the reptation model in two dimensions. Thus, if one accepts the reptation ansatz, the observed⁵ $D \sim N^{-3/2}$ follows naturally from the universal scaling of the reptation relaxation time, $\tau_D \sim N^3$, which combined with $R_G \sim N^{3/4}$ gives the diffusion coefficient,

$$D \sim R_G^2/\tau_D \sim N^{-1.5}. \quad (1)$$

The “tube” concept, which is central to the reptation ansatz, is, however, not obvious in this situation where the polymer surface coverage is dilute. In the simulation reported below, we have implemented the interpretation that a polymer chain diffuses through tortuosity presented by randomly spaced obstacles through which they cannot pass.

Several researchers previously addressed the issue of polymer dynamics in two dimensions via modeling approaches. Carmesin and Kremer⁸ presented a detailed analysis of dense linear two-dimensional polymer chains exhibiting Rouse behavior. Monte Carlo simulations of Azuma and Takayama⁹ for a single self-avoiding chain diffusing among regularly spaced impenetrable obstacles in two dimensions obtained the expected scaling of $D \sim N^{-1.5}$. Slater and Wu¹⁰ also used Monte Carlo simulations, but for 2D chain diffusion between randomly spaced obstacles. In contrast to Azuma and Takayama they found that the magnitude of the scaling exponent varied over the range of -1 to -2.39 depending on the obstacle concentration. While these results are interesting, the mapping between a Monte Carlo (MC) move and real time is not rigorously quantifiable. By contrast, the molecular-dynamics (MD) method provides detailed and unambiguous information of the time dependence of the dynamic properties of the system.

Seeking to systematically build upon these previous simulations, in this paper we report the results of molecular- and Brownian-dynamics simulations of single polymer chain diffusion in two dimensions in the presence of randomly placed impenetrable obstacles as a function of obstacle concentration. While these simulations properly account for the time scales of the dynamic processes, we completely ignore the hydrodynamic interactions due to the presence of explicit solvent. This is because in two dimensions, Falck *et al.*¹¹ showed theoretically and from simulations that the diffusion coefficient follows the form $D \sim \ln(L/R_G)$ where L is the system size. This logarithmic dependence of D on chain length with increasing system size is inevitable, and comes from the superdiffusive nature of motion in a 2D solvent arising from the inverse time t^{-1} asymptotic decay of the velocity autocorrelation function in 2D.¹² Thus, diffusion constants are truly undefined in the thermodynamic limit in 2D. In this case, the presence of the surface might serve as a means of momentum dissipation and thus circumvent this problem: this is a point that needs to be verified. With these

caveats, we shall study the transport properties of chains in two dimensions with the understanding that real experimental systems considered by Granick and Rädler are not truly 2D systems, but rather are three dimension (3D) systems including hydrodynamic interactions. Elsewhere we will describe simulation studies that allow segments of adsorbed polymer chains to form loops that dangle off the surface in the presence of explicit solvent.¹³ This introduction of the third dimension is computationally more expensive and presents the further disadvantage that it introduces additional parameters into the simulation model. The study reported below focuses on the specific case of diffusion strictly in two dimensions.

II. SIMULATION MODEL AND PROCEDURE

The two-dimensional MD simulations employ the bead-spring polymer chain model of Bird *et al.*,¹⁴ Kremer and Grest,¹⁵ and Rudisill and Cummings.¹⁶ The interaction energy between pairs of monomers is described by a purely repulsive potential derived by truncating and shifting a Lennard-Jones (LJ) potential at its minimum: $U(r) = 4\epsilon[(\sigma/r)^{12} - (\sigma/r)^6] + \epsilon$ for $r < 2^{1/6}\sigma$, and $U(r) = 0$ for $r > 2^{1/6}\sigma$. This potential is also known as the Weeks-Chandler-Anderson (WCA) potential.¹⁷ All lengths are reported in units of σ . Adjacent bonded monomers interact via a stiff finitely extendable nonlinear elastic (FENE) potential,¹⁸ which constrains the bond length to $\sim 1\sigma$. The combined effect of the LJ and FENE potentials prevents the chain from crossing itself. Thus, in the majority of MD simulations, a single self-avoiding chain is studied. The length of the chain is systematically varied in the range $N=6-160$ in a series of simulations. Periodic boundary conditions are employed in both directions. The system size studied in these simulations ranges from 62.5σ to 190σ .

The chain is placed in the plane containing randomly spaced, impenetrable, and immobile obstacles. The LJ interactions between the monomers and the obstacles are the same as between chain monomers, rendering the size of the obstacles to be the same as that of the monomer. Simulations are carried out for various obstacle concentrations c , defined as $c = N_o/L^2$, where N_o = number of obstacles and L = simulation box length.

We used the standard predictor-corrector¹⁹ algorithm to integrate the equations of motion with a time step of 0.005τ , where $\tau = \sigma(m/\epsilon)^{1/2}$. The temperature is maintained by the application of an additional stochastic force as in the work of Kremer and Grest.¹⁵ The viscous drag parameter is adjusted to a value such that the mean free path of the polymer chain without obstacles is a small fraction of the monomer size. The amplitude of the stochastic noise (via the dissipation fluctuation theorem) is such that the temperature is set to $T^* = T/(\epsilon/k_B) = 0.5$, where k_B is Boltzmann's constant. This model of the solution corresponds to the standard “vacuum solvent” description under good solvent conditions. Hence the polymer-solvent (hydrodynamic) interactions are neglected.

The structures were equilibrated over a time interval such that each chain has moved at least twice its radius of

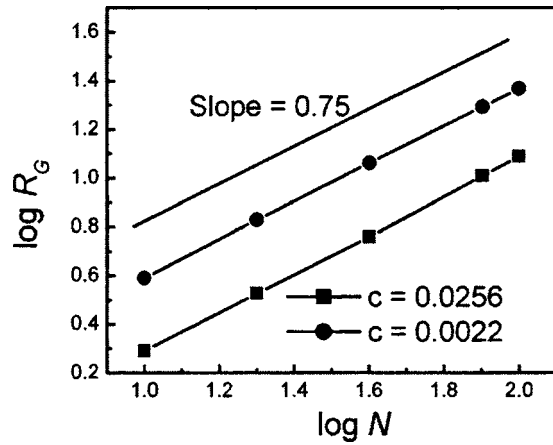


FIG. 1. Comparison of the rms radius of gyration R_G of the polymer chain at two extreme obstacle concentrations, $c=0.0256$ and $0.0022/\sigma^2$. The R_G values are plotted as a function of chain length, N , on a log-log scale. The R_G values for the $c=0.0022$ are shifted vertically for better visualization. The R_G values are same for both obstacle concentrations.

gyration R_G . Such equilibrated structures are then initial structures for production runs of $(40-400)\tau \times 10^6$ MD steps over which we collect the structural and dynamical data. The averaging was carried out for several realizations at each c , the obstacle concentration.

III. RESULTS

This section describes the results of simulations of polymer chain diffusion in the presence of obstacles whose concentrations range from $c\sigma^2=0$ to 0.0256 . We first analyze the structural characteristics, especially focusing on the size of the polymer chain radius of gyration R_G . The scaling result for the dependence of R_G on chain length is $\langle R_G^2 \rangle^{1/2} \sim N^\nu$, where $\nu=3/(d+2)$, i.e., $\nu=0.75$ in two dimensions.¹ In Fig. 1, we show R_G values averaged over the simulation run for the two extreme cases of obstacle concentration, $c=0.0022$ and $0.0256/\sigma^2$. The R_G values are plotted as a function of N on a log-log scale. The slope of 0.75 ± 0.03 , apparently independent of obstacle concentration, confirms the scaling result.

Although not apparent in this representation, we find that not only does the slope not depend on c but the absolute values of R_G are virtually identical for all concentrations studied. This result indicates that the concentration of obstacles in our studies is too low to alter chain structure. In fact, for the highest obstacle concentration studied, the po-

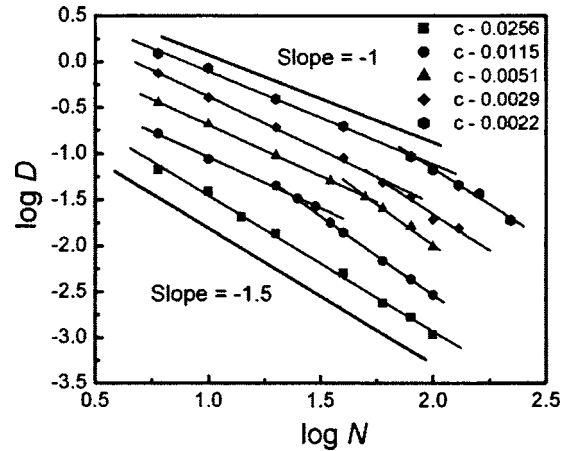


FIG. 2. The self-diffusion coefficient D of the polymer chain is plotted as a function of chain length N on a log-log scale for a selection of obstacle concentrations. The values of D are shifted for better visualization. We see a cross over from Rouse to reptation regime for various obstacle concentrations.

rosity is about 97%. On physical grounds we expect that, if the obstacle concentration were sufficiently large, the chains would contract and eventually collapse.

To understand the effect of low obstacle concentrations on the dynamical properties of the chain, we measured the diffusion coefficient of the chain center of mass. We analyze the mean-square displacement of the center of mass of chains,

$$g_3(t) = \langle [r_{c.m.}(t) - r_{c.m.}(0)]^2 \rangle, \quad (2)$$

where t is the time, and the outer brackets denote averaging over different time origins. The diffusion coefficient D results from the application of the Einstein equation for 2D: $g_3(t) = 4Dt$. Figure 2 shows diffusion coefficient values as a function of chain length N for a selection of obstacle concentrations on a log-log scale. The average distance S , where $S = (1/c)^{0.5}$, between randomly spaced obstacles ranges from ∞ (no obstacles) to 6.25σ .

Since we apply a stochastic force on each chain bead, we verified that the polymer chain exhibits Rouse-type behavior ($D \sim N^{-1}$) in the absence of obstacles. For nonzero obstacle concentrations the transition from Rouse behavior to reptation is clearly seen in Fig. 2. For all concentrations the crossover is from a scaling exponent of -1 to -1.5 , independent of obstacle concentration.¹⁰

From Fig. 2 we can estimate the chain length at which the crossover from the Rouse to reptation behavior takes

TABLE I. Obstacle concentration c , crossover chain length, the interpolated radius of gyration R_G and the end-to-end distance R_e for a chain of the crossover length, the distance between obstacles S , and the ratio (R_e/S) estimated from Fig. 2. The ratio of (R_e/S) of 1–1.2 indicates that crossover takes place when the distance between obstacles is approximately equal to the R_e of the chain.

c	Crossover chain length	R_G	R_e	S	R_e/S
0.0115	22	3.63 ± 0.3	9.34 ± 0.7	9.31	1.00 ± 0.07
0.0051	50	6.82 ± 0.6	17.6 ± 0.8	13.97	1.25 ± 0.06
0.0029	63	7.97 ± 0.75	21.0 ± 1.7	18.63	1.12 ± 0.09
0.0022	80	10.19 ± 0.6	25.2 ± 2	20.96	1.20 ± 0.09

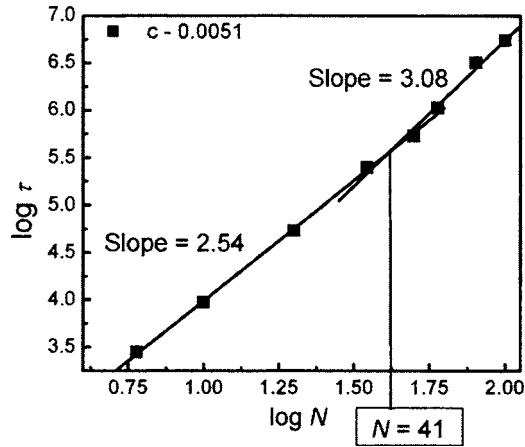


FIG. 3. The longest relaxation time τ calculated from the autocorrelation function of the end-to-end vector plotted as a function of chain length N on a log-log scale. The Rouse and reptation models predict $\tau \sim N^{2.5}$ and $\tau \sim N^3$, respectively. The plot matches these predictions and we see a crossover at $N \sim 40$.

place, i.e., the chain length at which the slopes intersect. For the highest obstacle concentration, the polymer chain lies in the reptation regime for all values of N studied. For all other c values we tabulate the obstacle concentration, the corresponding crossover chain length, the end-to-end distance for this chain length, R_e , the distance between obstacles, S , and the ratio R_e/S in Table I. The ratio of end-to-end distance R_e to distance between the obstacles at the crossover is approximately 1, apparently independent of c . This provides a nice physical interpretation of the crossover in behavior that is observed.

To further analyze this crossover in dynamical behavior, for obstacle concentration of $c=0.0051/\sigma^2$ we calculate the longest chain relaxation time τ from the autocorrelation function of the end-to-end vector: $P(t)=\langle R(t) \cdot R(0) \rangle \sim \exp[-(t/\tau)]$. Figure 3 shows this τ as a function of chain length N on a log-log scale. The slope for smaller chains, below the crossover, is 2.54 and for chains above the crossover is 3.08. This satisfies the expected relaxation time dependence for both regimes: $\tau \sim (R_e)^2/D$, suggesting that we have internal consistency in our findings. The length estimated from the crossover in the scaling behavior of the end-to-end vector relaxation time (see Fig. 3) is equal to $N \sim 40$, which is close to that estimated from the diffusion, $N \sim 50$ (see Fig. 2 and Table I).

Azuma and Takayama showed that for a self-avoiding polymer embedded in regularly distributed obstacles and confined in two dimensions, the mean-square displacement of a center monomer $g_1(t)$ exhibits four dynamical regimes, i.e., $g_1(t) \sim t^\nu$ with $\nu \sim 0.6, 0.375, 0.75$, and 1 from the shortest- to longest-time regime, respectively. In Fig. 4 we plot the time dependence of the mean-square displacement of the five monomers at the center, on a log-log scale for a polymer chain of $N=80$ and at an obstacle concentration of 0.0256. The plot is in agreement with the theoretical and MC simulations for the power-law dependences, except for the second regime, where we get a slightly higher slope of ~ 0.45 rather than 0.375. Similar deviations were observed by Azuma and Takayama for a chain length of $N=100$.

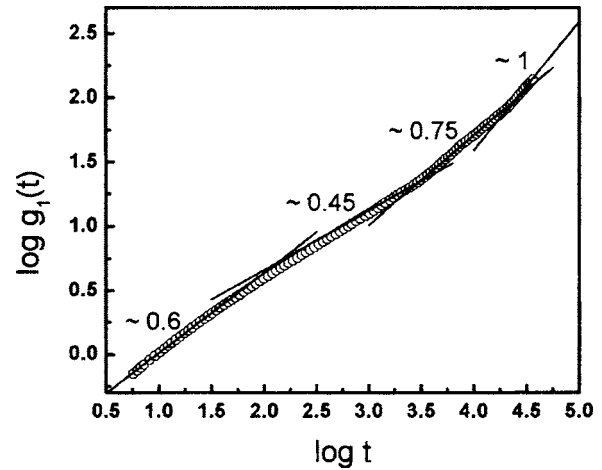


FIG. 4. Time dependence of mean-square displacement of the single monomer $g_1(t)$ averaged over the five inner monomers of a chain of $N=80$ and obstacle concentration of 0.0256 on a log-log scale.

In the Rouse model, the mean-square displacement of any monomer along the chain increases with time as $\langle r^2(t) \rangle \propto t^{0.6}$ in two dimensions. This also shows up in the incoherent structure factor.

$$S_{\text{inc}}(k,t) = \exp \left[-\frac{1}{6} k^2 \langle r^2(t) \rangle \right], \quad (3)$$

where k is the wave vector. For large wave vectors, the internal dynamics of the chain are probed rather than overall, diffusive motion.²⁰ The reptation model predicts a $t^{0.375}$ law for values of k smaller than the inverse tube diameter in two dimensions. In our case the tube diameter is proportional to the average separation distance between obstacles. In Fig. 5 we plot $-\ln(S_{\text{inc}}(k,t))$ for two different k values of 0.45 and 0.9. The incoherent structure factor is calculated for the central monomer of the chain. In both cases we find an initial slope of ~ 0.65 representing the Rouse behavior and then a crossover to ~ 0.38 following the reptation model. We also plot the incoherent structure factor for the case of infinite separation distance between the obstacles in Fig. 5. No such crossover is seen in the scaling behavior, thus identifying it

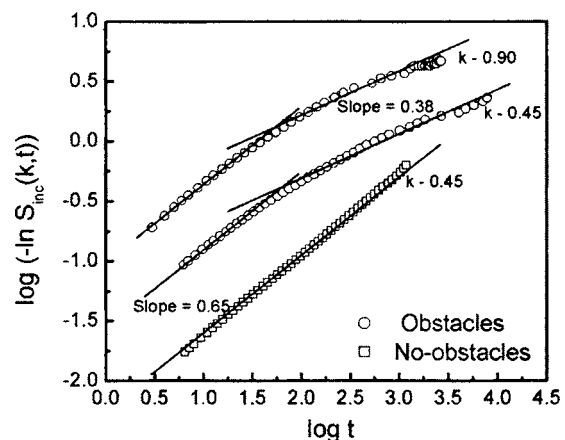


FIG. 5. Incoherent structure factor $-\ln(S_{\text{inc}}(k,t))$ plotted as a function of time on log-log scale for $k=0.45$ and 0.9 and obstacle concentration $c=0.0256$ and for $k=0.45$ and no obstacles. The incoherent structure factor is calculated only for the center monomer of the chain of length $N=80$.

as being a consequence of the obstacles. In this case we found only two-time regimes, i.e., $\nu \sim 0.6$ and 1, a characteristic of Rouse behavior for the situation with no obstacles.

IV. DISCUSSION AND CONCLUSIONS

From these simulations of 2D polymer diffusion at a solid surface, performed over a wide range of N , the main point that emerges is that the motion of chains changes from Rouse-type to reptationlike when the mean separation between obstacles was approximately equal to the 2D end-to-end distance. Simulations of systems with the third dimension and explicit solvent to include hydrodynamic interactions are probably needed to make explicit contact with experiment; however, the current findings suggest strongly the paramount importance of surface obstacles in rate limiting the translation diffusion of chains at solid surfaces.

Looking to the future, it is interesting to speculate how the consequences of surface disorder, interpreted here for the specific instance of literal obstacles, may generalize when seeking to apply these ideas to the natural world. From a survey of the chemical and topographical makeups of natural surfaces, one quickly appreciates that the notion of having a solid surface with uniform affinity for polymer adsorption is probably very rare in the natural world. There is disorder in the form of topography and physical roughness; also there is disorder in the form of chemical unevenness, such that the sites of potential polymer adsorption are unevenly distributed on a surface, and furthermore distributed with uneven intensity.

From the obstacle disorder that forms the specific subject of these simulations, to the additional types of surface disorder just mentioned, the conceptual path is clear by rational extension. Although the study presented here concerns only a single type of surface disorder, we suggest tentatively that

the profound distinction between having a smooth and a disorderly surface may underlie the mechanism of polymer surface diffusion.

ACKNOWLEDGMENTS

We acknowledge the financial support of the National Science Foundation through Grant Nos. CMS-0310596 and DMR-0413755 and The National Science Foundation Nanoscale Science and Engineering Center at RPI, NSF Grant No. DMR-0117792. S.G. acknowledges support from the U.S. Department of Energy, Division of Materials Science, Grant No. DEFG02-02ER46019.

¹P. G. de Gennes, *Scaling Concepts in Polymer Physics* (Cornell University Press, Ithaca, 1985).

²M. Doi and S. F. Edwards, *The Theory of Polymer Dynamics* (Clarendon, Oxford, 1986).

³B. H. Zimm, *J. Chem. Phys.* **24**, 269 (1956).

⁴P. E. Rouse, *J. Chem. Phys.* **21**, 1272 (1953).

⁵S. A. Sukhishvili, Y. Chen, J. D. Muller, E. Gratton, K. S. Schweizer, and S. Granick, *Nature (London)* **406**, 146 (2000); S. A. Sukhishvili, Y. Chen, J. D. Muller, E. Gratton, K. S. Schweizer, and S. Granick, *Macromolecules* **35**, 1776 (2002).

⁶B. Maier and J. O. Radler, *Phys. Rev. Lett.* **82**, 1911 (1999); B. Maier and J. O. Radler, *Macromolecules* **33**, 7185 (2000).

⁷L. Zhang and S. Granick, *Proc. Natl. Acad. Sci. U.S.A.* **102**, 9118 (2005).

⁸I. Carmesin and K. Kremer, *J. Phys. (France)* **51**, 915 (1990).

⁹R. Azuma and H. Takayama, *J. Chem. Phys.* **111**, 8666 (1999).

¹⁰G. W. Slater and S. Y. Wu, *Phys. Rev. Lett.* **75**, 164 (1995).

¹¹E. Falck, O. Punkkinen, I. Vattulainen, and T. Ala-Nissilä, *Phys. Rev. E* **68**, 050102(R) (2003); O. Punkkinen, E. Falck, I. Vattulainen, and T. Ala-Nissilä, *J. Chem. Phys.* **122**, 094904 (2005).

¹²B. J. Alder and T. E. Wainwright, *Phys. Rev. A* **1**, 18 (1970).

¹³T. G. Desai, P. Keblinski, S. K. Kumar, and S. Granick (unpublished).

¹⁴R. B. Bird, C. F. Curtiss, R. C. Armstrong, and O. Hassager, *Dynamics of Polymeric Liquids: Kinetic Theory* (Wiley, New York, 1987), Vol. 2.

¹⁵G. S. Grest and K. Kremer, *Phys. Rev. A* **33**, 3628 (1986).

¹⁶J. W. Rudisill and P. T. Cummings, *Rheol. Acta* **30**, 33 (1991).

¹⁷J. D. Weeks, D. Chandler, and H. C. Anderson, *J. Chem. Phys.* **54**, 5237 (1971).

¹⁸G. S. Grest and K. Kremer, *J. Chem. Phys.* **92**, 5057 (1990).

¹⁹M. P. Allen and D. J. Tildesley, *Computer Simulations of Liquids* (Clarendon, Oxford, 1986).

²⁰D. Richter, A. Baumgartner, and K. Binder, *Phys. Rev. Lett.* **47**, 109 (1981).